

A New Mode Stirrer Design for the Reverberation Chamber

Jiazhi Tang¹, Furong Li¹, Junhao Zheng¹, Xiaoming Chen¹, Yingsong Li^{2,3}, and Juan Chen⁴

¹School of Information and Communications Engineering
Xi'an Jiaotong University, Xi'an, 710049, China
furong.li@xjtu.edu.cn

²College of Information and Communication Engineering
Harbin Engineering University, Harbin, 150001, China

³Key Laboratory of Microwave Remote Sensing
National Space Science Center, Chinese Academy of Sciences, Beijing, 100190, China

⁴Shenzhen Research School
Xi'an Jiaotong University, Shenzhen, 518057, China

Abstract — In this paper, a mode stirrer composed of random positioned metal plates is proposed for reverberation chamber. The designing procedure of the mode stirrer is presented. The designed stirrer is compared with the common Z-shaped stirrer in both simulation and measurement. It is shown that in general the proposed stirrer outperforms the common Z-shaped stirrer with the same sweeping volume. Nevertheless, the measurement results show that the performance improvement of the designed stirrer becomes insignificant at higher frequencies with additional platform stirring. Albeit the difference, the stirring improvement of the designed stirrer is clearly demonstrated at low frequencies, which is more important due to the inherent low mode density at low frequency.

Index Terms — Independent sample number, measurement uncertainty, mode stirrer, reverberation chamber.

I. INTRODUCTION

The reverberation chamber is a shielded room with various stirring mechanisms for over-the-air (OTA) and electromagnetic compatibility (EMC) tests [1]. Whether the electromagnetic fields are statistically homogeneous and isotropic or not is of great importance to the reverberation chamber testing. Due to the stochastic nature of reverberation chamber measurements, measurement uncertainty analysis is of great importance for EMC/OTA tests in the reverberation chamber [2]-[7]. Experimental evaluation of the measurement uncertainty dictates many independent and repeated measurements. To avoid the time-consuming uncertainty characterization, one can resort to the equivalent number of independent samples

N_{ind} , which is related to the standard deviation (uncertainty) σ as $\sigma = 1/\sqrt{N_{ind}}$ [6]. The advantage of using N_{ind} is that, instead of conducting many sets of independent measurements, one can estimate N_{ind} from one set of measurement [2],[6]. The measurement uncertainty and the field uniformity are equivalent for evaluating the stirring performance of the reverberation chamber. As a result, many studies use the number of independent samples (or a slightly different form of it) to evaluate the stirring performance in the reverberation chamber, e.g., [7]-[11]. Hence, we will use the same performance indicator in this work.

There are complicated factors affecting the electromagnetic field distribution in the reverberation chamber, including mode stirrer, turntable platform, and scatters on the metal walls. Many works are carried out to optimize these factors to reduce the measurement uncertainty, e.g., stirrer [12],[13], diffusors [14],[15], turntable platform [16] or source stirring [17],[18], metasurface for changing the cavity boundary condition [19]-[21].

In this work, we use a random optimization algorithm to optimize the mode stirrer. The optimized stirrer is fabricated and measured in a reverberation chamber. Superior performance to the conventional Z-shaped stirrer is observed by both simulation and measurement. This is especially true at low frequencies. However, it is shown from measurement result that with platform stirring, the superior performance of the designed stirrer vanish at higher frequencies. Explanation and verification are given. Nevertheless, since the inherent mode density of the reverberation chamber increases with frequency, it is more important to improve the

measurement uncertainty at the lowest usable frequency. Therefore, the designed stirrer proves to be useful for practical reverberation chamber measurements.

II. DESIGN OF STIRRER

There are in general two types of mode stirrers: rotating stirrer and translating stirrer. It was found that the rotating stirrer not only enjoys simpler motor structure but also has better stirring performance as compared with the translating stirrer, provided that the sweeping volume of the two types of mode stirrers are the same [15]. Therefore, this work focuses solely on the rotating stirrer.

The (rotating) stirrer in a reverberation chamber is usually composed of a central axis, several metal plates, and an electric motor. It can be seen in Fig. 1 (a) that the metal plates of Z-shape stirrer are stitched one by one with a uniform 120 degree flare angle (except at the top and bottom). Note that each metal plate shall be no less than one quarter of the wavelength at the lowest usable frequency [2].

For comparison fair in this work, we set the sweeping volume of all the stirrers to be $0.2\text{ m} \times 0.2\text{ m} \times 1.2\text{ m}$. The initial state of the stirrer to be optimized is shown in Fig. 1 (b). There are in total 196 metal plates each with a size of $10\text{ mm} \times 10\text{ mm}$. Obviously, the stirrer shown in Fig. 1 (b) will be inefficient for mode stirring in a reverberation chamber due to its symmetry around the rotating axis. Hence, for optimal stirring performance, we should make it asymmetric and irregular.

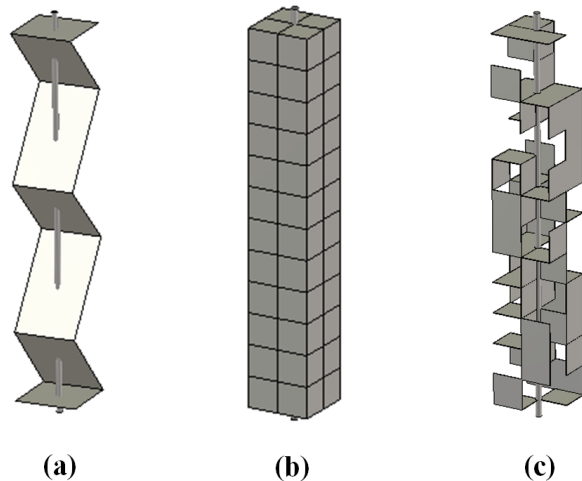


Fig. 1. Models of stirrers: (a) Z-shape stirrer, (b) initial state of the stirrer to be optimized, and (c) optimized stirrer.

By applying the genetic algorithm (GA) [12] to optimize the stirrer, the final design of the stirrer is depicted in Fig. 1 (c). Such an irregular design can be intuitively explained via Fig. 2, from which it can be seen that merely several metal plates can form different metal

structures. Under different incident wave directions, different metal structures result in different wave reflections and diffractions. Therefore, the whole stirrer can be designed by using many such metal cavities with random positions. In order to simplify the design procedure, coding ideas are applied. According to the binary theory, the 196 metal plates are converted into a 196-bit code composed of 1 and 0 codes. When constructing the stirrer, 0 means that the corresponding position of the stirrer is empty, while 1 means that there is a corresponding metal plate at that position.

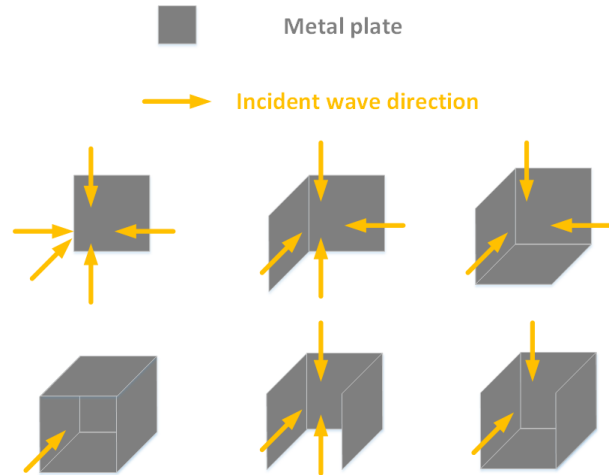


Fig. 2. Different metal plate structures with different incident wave directions.

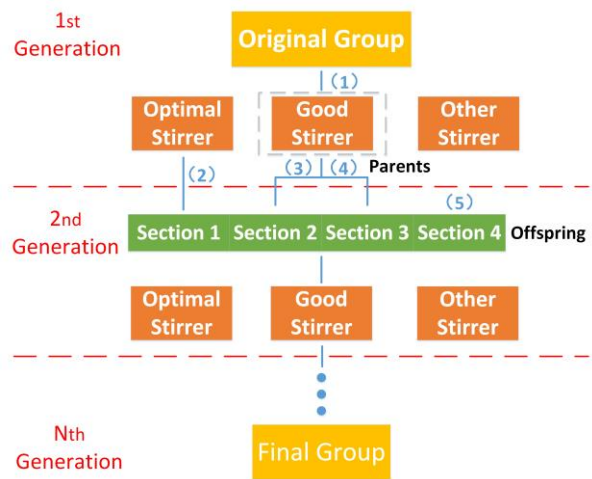


Fig. 3. Optimization process of stirrer through the genetic algorithm.

The optimization process is accomplished through co-simulations with Matlab and CST full wave simulation software, where the evaluation of each stirrer is carried through in CST and all the data processing as well as the optimization algorithm are conducted in Matlab. The

whole procedure is depicted in Fig. 3, which mainly demonstrates how the first generation evolves into the second generation. Note that in the optimization algorithm the stirrer is regarded as the chromosome while the 196 metal plates are the genes. At the beginning of the procedure, 50 stirrers that are randomly generated constitute the original group (cf. orange color box) and there are 5 steps in its evolution into next generation (cf. green color boxes): 1) evaluate all members in the original group ranking from the best to the worst, where the optimal stirrer is the top one, the good stirrers are the 2nd-10th members in rank and the other stirrers are the rest; 2) the optimal stirrer is chosen directly as section 1 of the offspring; 3) two individuals from good stirrers are selected as parents according to probability (calculated from the rank) and provide their genes (half of each one's genes for crossover) to form one offspring. 19 new stirrers are constructed like this in section 2; 4) there are 20 new stirrers born in section 3 and every offspring get its genes as in step 3), whereas 5% of its genes are chosen to mutate (random gene locations); 5) 10 stirrers are randomly generated in section 4 to maintain the population diversity. Finally, in total 50 offspring from the four sections become the second generation. In fact, these steps are the so-called evaluation fitness, natural selection, mate selection, mutation and offspring generating in the GA. When repeating the 5 steps, the second, third and N_{th} generation with 50 stirrers can be acquired until the optimization is converged [12]. Next, the evaluation process will be illustrated in the following paragraph.

To evaluate the performance of the coded stirrer, a top view of schematic diagram is shown in Fig. 4. The stirrer (blue square) is located in the center and spherical uniform incident wave (grey dotted circle line) is generated impinging on it. Field probes are set surrounding the stirrer to observe the reflected wave. E and H field values recorded by the probes are used to calculate the average angle of the Poynting vector $\theta_{Ave_poynting}$, which signifies a measure of the ability of changing the electromagnetic field distribution. Through the GA algorithm optimization in Fig. 3, the proposed stirrer can be obtained and the comparison of the mean angle of the Poynting vector has been exhibited in Table 1. As can be seen, the optimized stirrer (cf. Fig. 1 (c)) has the highest value, whereas the initial state of the stirrer (cf. Fig. 1 (b)) has the lowest value as expected. From Table 1, it can be inferred that the optimized stirrer has the best stirring performance. By applying this stirrer in a reverberation chamber, the electromagnetic field will be stirred more efficiently and its distribution can become more uniform from a statistical point of view.

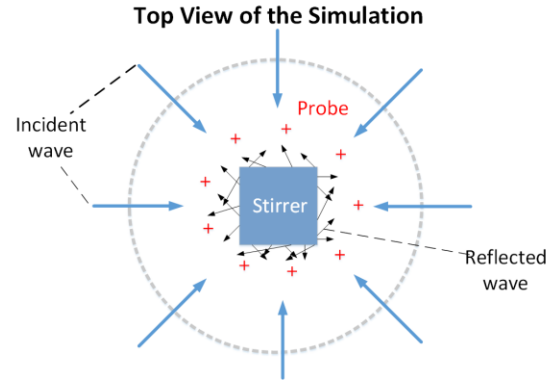


Fig. 4. Model to evaluate the stirrer.

Table 1: Average angle of the Poynting vector

Stirrer	$\theta_{Ave_poynting}$
Z-shape	7.64
Original	5.25
Final	12.73

III. SIMULATIONS

The reverberation chamber used for simulation has a size of 1.44 m × 0.92 m × 1.5 m as shown in Fig. 5. The dimensions are chosen to be the same as the reverberation chamber in the Lab. In this model, the transmit antenna is a discone antenna (red color) placed in the corner, while the stirrer is located vertically around the z-axis. Furthermore, the working volume is set as 0.4 m × 0.52 m × 0.3 m with 8 field probes (black cross figure) at its 8 vertices to sample the electric field. (Each probe can sample three orthogonal rectangular components of the E field.) The testing frequency range is from 1 to 2 GHz. Given the chamber's dimensions, one can readily find out that the lowest usable frequency of the reverberation chamber is around 1 GHz [2].

The simulation is also carried out in the CST full wave simulation software. During the simulation, the proposed stirrer rotates stepwise around the vertical axis with an angular step of 6°. The 8 electric probes record the rectangular components of E field at each rotation angle of the stirrer. After 60 rotations, the sampled data of probes are collected and analyzed. To evaluate the stirrer's stirring performance, the number of independent samples of test is calculated by the auto-correlation function (ACF) method [6]. According to the ACF method, the n -th auto-correlation coefficient is calculated by:

$$\rho_n = \frac{\sum_{i=1}^{N-1} (x_i - \langle x \rangle)(x_{i+n} - \langle x \rangle)}{(N-1)\sigma^2}, \quad (1)$$

where x is the recorded data, σ^2 is the variance of x :

$$r = \frac{1}{e} \left(1 - \frac{7.22}{N^{0.64}} \right), \quad (2)$$

where e is the base of the natural logarithm function ($e \approx 2.7183$) [2] and r is the threshold of the auto-correlation coefficient of the measured samples [7] and often equal to 0.37. The offset number $N_{\Delta,i}$ is determined from the ACF using the threshold. The number of independent samples of the data is then determined as:

$$N_{ind,i} = \frac{N}{N_{\Delta,i}}, \quad (3)$$

where i ranges from 1 to 24 (8 probe locations \times 3 electric field rectangular components) and $N = 60$ is the whole rotation sample number. Finally, the averaged number of independent samples over all the probes N_{all} is calculated as:

$$N_{all} = \frac{\sum_{i=1}^{24} N_{ind,i}}{24}. \quad (4)$$

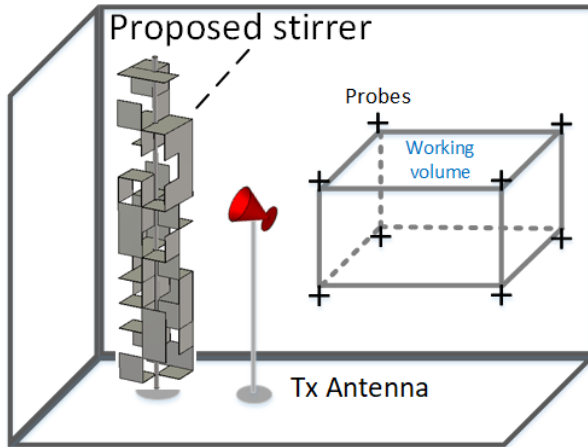


Fig. 5. Simulation model of stirrer in reverberation chamber.

The simulation procedure is repeated for the optimized stirrer and a common Z-shaped stirrer, respectively. For fair comparison, the sweeping volume of the two stirrers are set to be the same. Their stirring performances are compared in Fig. 6. The black line represents the number of independent samples corresponding to the Z-shaped stirrer, while the red color line stands for the number of independent samples corresponding to the optimized stirrer. Note that due to the stochastic nature of the reverberation chamber, both curves are fluctuated and a 50-MHz smoothing windows is applied to make them more readable [6]. Nevertheless, it is obvious that the value of the red line apparently larger than that of the black line over the entire frequency range. This implies that the optimized stirrer clearly

outperforms the common Z-shaped stirrer.

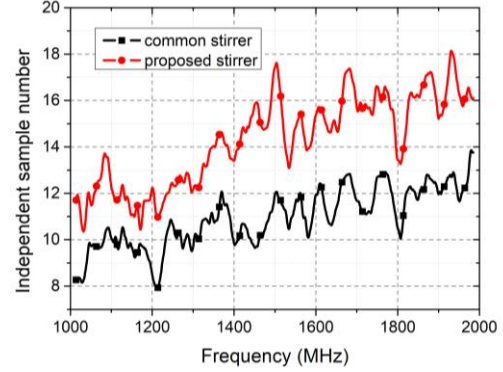


Fig. 6. Comparison of numbers of independent samples of simulated reverberation chamber with the two different stirrers.

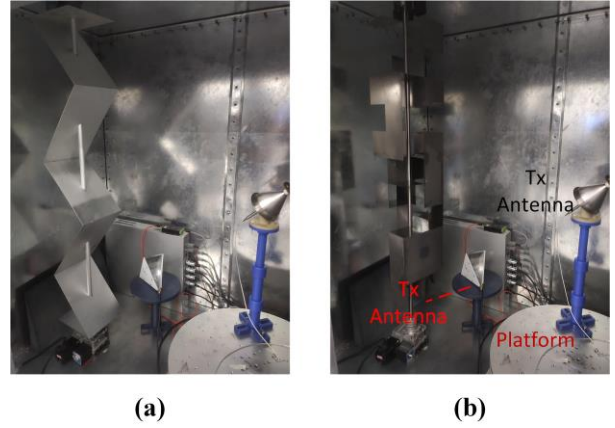


Fig. 7. Measurement setup of reverberation chamber with: (a) Z-shaped stirrer and (b) optimized stirrer.

IV. MEASUREMENTS

The used reverberation chamber for actual measurements is located at the Xi'an Jiaotong University, Xi'an, China. The proposed stirrer is manufactured and installed in the reverberation chamber as shown in Fig. 7. The reverberation chamber is mainly equipped with a turntable platform, a transmit antenna, and a receive antenna. In the measuring process, the stirrer and turntable platform are controlled by a personal computer (PC). A vector network analyzer is used to collect the data from the two antennas. The sampling number of the test is 100 (10 stirrer rotation angles \times 10 platform rotation angles).

Figure 8 shows the estimated numbers of independent samples (solid curves) with the Z-shaped stirrer and the optimized stirrer together. As can be seen, the number of independent samples of optimized stirrer is larger than that of the Z-shaped stirrer below 1.6 GHz. Above 1.6 GHz, the two stirrers have essentially the same

stirring performance. The different trends between the measurement and simulation in Fig. 5 are attributed to several factors: 1) the boundary condition of the actual reverberation chamber is much more complicated than that of the simulated chamber; 2) the actual chamber is equipped with a turn-table platform that is missing in the simulation due to computational complexity; 3) it has been found experimentally that platform stirring is more effective than mode stirring [22]. The last factor is probably the dominant one, because once the distance between two consecutive positions of the antenna on the platform is larger than the coherence distance [10] (which is the case at higher frequencies), the stirring performance is dominated by the platform stirring and the stirrer performance improvement becomes insignificant. To verify the analysis, another simulation including the platform stirring condition is conducted and the results are also exhibited in Fig. 8 (dotted curves). It is noted that the two dotted lines above 1.55 GHz have smaller difference than that below 1.55 GHz, which is in accordance with the measurement curves. Hence the additional simulation results substantiate that the third factor is the main cause of the difference of solid lines between Fig. 6 and Fig. 8. Nevertheless, as mentioned before, for reverberation chamber measurements it is most challenging and important to improve the stirring performance around the lowest usable frequency. The stirring performance at higher frequencies are good anyway due to the inherent mode density of the reverberation chamber that increases with frequency. Thus, it is highly desirable to have such a stirrer (cf. Fig. 1 (c)) that can improve the stirring performance at lowest usable frequency.

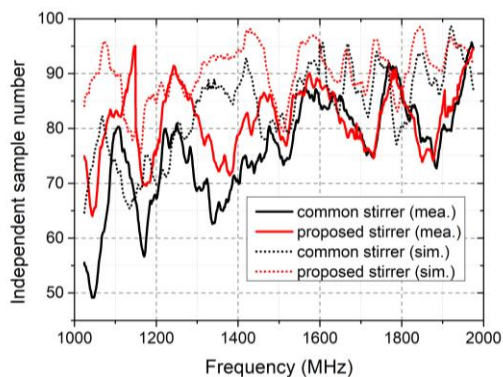


Fig. 8. Comparison of numbers of independent samples of measurements (solid curves) and simulations (dotted curve) of the two different stirrers with platform.

V. CONCLUSION

In this paper, an optimized stirrer was presented. Its superior performance was demonstrated by simulation as well as measurement. The differences between simulation and measurement was explained. It was shown that the

optimized stirrer could improve the stirring performance of the reverberation chamber around the lowest usable frequency. At higher frequency, however, the stirring performance was dominated by the turntable platform. Nevertheless, as explained in the paper, it was of great importance to have such an optimized stirrer to improve the performance of the reverberation chamber at low frequencies, where the mode density was inherently low.

ACKNOWLEDGMENT

This work was supported in part by the National Natural Science Foundation of China under Grants 61801366 and the Natural Science Foundation of Shaanxi Province under Grant 2020JM-078, and by Technology Program of Shenzhen (grant number JCYJ20180508152233431).

REFERENCES

- [1] X. Chen, J. Tang, T. Li, S. Zhu, Y. Ren, Z. Zhang, and A. Zhang, "Reverberation chambers for over-the-air tests: An overview of two decades of research," *IEEE Access*, vol. 6, pp. 49129-49143, Aug. 2018.
- [2] IEC 61000-4-21: Electromagnetic Compatibility (EMC), Part 4-21: Testing and Measurement Techniques - Reverberation Chamber Test Methods. *Int. Electrotech Comm.*, Edition 2.0, 2011.
- [3] A. Gifuni, I. D. Flintoft, S. J. Bale, G. C. R. Melia, and A. C. Marvin, "A theory of alternative methods for measurements of absorption cross section and antenna radiation efficiency using nested and contiguous reverberation chambers," *IEEE Trans. Electromagn. Compat.*, vol. 58, no. 3, pp. 678-685, June 2016.
- [4] M. Barazzetta, D. Micheli, L. Bastianelli, R. Diamanti, M. Totta, P. Obino, R. Lattanzi, F. Moglie, and V. Mariani Primiani, "A comparison between different reception diversity schemes of a 4G-LTE base station in reverberation chamber: A deployment in a live cellular network," *IEEE Trans. Electromagn. Compat.*, vol. 59, no. 6, pp. 2029-2037, Dec. 2017.
- [5] K. A. Remley, R. J. Pirkl, C. Wang, D. Senić, A. C. Homer, M. V. North, M. G. Becker, R. D. Horansky, and C. L. Holloway, "Estimating and correcting the device-under-test transfer function in loaded reverberation chambers for over-the-air tests," *IEEE Trans. Electromagn. Compat.*, vol. 59, no. 6, pp. 1724-1734, Dec. 2017.
- [6] X. Chen, "Experimental investigation of the number of independent samples and the measurement uncertainty in a reverberation chamber," *IEEE Trans. Electromagn. Compat.*, vol. 55, no. 5, pp. 816-824, Oct. 2013.
- [7] N. Wellander, O. Lunden, and M. Bäckström, "Experimental investigation and mathematical

- modeling of design parameters for efficient stirrers in mode-stirred reverberation chambers,” *Trans. Electromagn. Compat.*, vol. 49, no. 1, pp. 94-103, Feb. 2007.
- [8] C. Lemoine, P. Besnier, and M. Drissi, “Estimating the effective sample size to select independent measurements in a reverberation chamber,” *IEEE Trans. Electromagn. Compat.*, vol. 50, no. 2, pp. 227-236, May 2008.
- [9] R. J. Pirkl, K. A. Remley, and C. S. L. Patané, “Reverberation chamber measurement correlation,” *IEEE Trans. Electromagn. Compat.*, vol. 54, no. 3, pp. 533-544, June 2012.
- [10] X. Chen, “On near-field and far-field correlations in reverberation chambers,” *IEEE Microw. and Wireless Compon. Lett.*, vol. 29, no. 1, pp. 74-76, Jan. 2019.
- [11] G. Gradoni, V. Mariani Primiani, and F. Moglie, “Reverberation chamber as a multivariate process: FDTD evaluation of correlation matrix and independent positions,” *Progress in Electromagnetics Research*, vol. 133, pp. 217-234, Jan. 2013.
- [12] J. Clegg, A. C. Marvin, J. F. Dawson, and S. J. Porter, “Optimization of stirrer designs in a reverberation chamber,” *IEEE Trans. Electromagn. Compat.*, vol. 47, no. 4, pp. 824-832, Nov. 2005.
- [13] Q. Xu and Y. Huang, *Anechoic and Reverberation Chambers: Theory, Design and Measurements*. Wiley-IEEE Press, 2018.
- [14] W. Petirsch and A. J. Schwab, “Investigation of the field uniformity of a mode-stirred chamber using diffusers based on acoustic theory,” *IEEE Trans. Electromagn. Compat.*, vol. 41, no. 4, pp. 446-451, Nov. 1999.
- [15] X. Chen, “Measurement uncertainty of RC and its reduction techniques for OTA tests: A review,” *IET Microw., Antennas, Propag.*, vol. 13, no. 15, pp. 2598-2604, May 2019.
- [16] X. Chen, “Scaling factor for turn-table platform stirring in reverberation chamber,” *IEEE Antennas and Wireless Propagat. Lett.*, vol. 16, pp. 2799-2802, Aug. 2017.
- [17] G. Cerri, V. Mariani Primiani, S. Pennesi, and P. Russo, “Source stirring mode for reverberation chambers,” *IEEE Trans. Electromagn. Compat.*, vol. 47, no. 4, pp. 815-823, Nov. 2005.
- [18] X. Chen, W. Xue, H. Shi, J. Yi, and W. E. I. Sha, “Orbital angular momentum multiplexing in highly reverberant environments,” *IEEE Microw. and Wireless Compon. Lett.*, vol. 30, no. 1, pp. 112-115, Jan. 2020.
- [19] L. Wanderlinder, D. Lemaire, I. Coccato, and D. Seetharamdoo, “Practical implementation of metamaterials in a reverberation chamber to reduce the LUF,” *IEEE 5th Int. Symp. Electromag. Compat.*, Beijing, China, Oct. 2017.
- [20] H. Sun, C. Gu, Z. Li, Q. Xu, J. Song, B. Xu, X. Dong, K. Wang, and F. Martín, “Enhancing the number of modes in metasurfaced reverberation chambers for field uniformity improvement,” *Sensor*, vol. 18, pp. 1-10, Sep. 2018.
- [21] J.-B. Gros and P. Hougne, “Tuning a regular cavity to wave chaos with metasurface-reconfigurable walls,” *Phys. Review A*, vol. 101, 061801(R), June 2020.
- [22] P.-S. Kildal, X. Chen, C. Orlenius, M. Franzén, C. and S. Lötbäck Patané, “Characterization of reverberation chambers for OTA measurements of wireless devices: physical formulations of channel matrix and new uncertainty formula,” *IEEE Trans. Antennas Propagat.*, vol. 60, no. 8, pp. 3875-3891, Aug. 2012.



Jiazhi Tang is currently pursuing the Ph.D. degree in Xi'an Jiaotong University. His research interest is metasurface and reverberation chamber.



Furong Li is a Research Assistant at Xi'an Jiaotong University, Xi'an, China.



Junhao Zheng is currently pursuing the Ph.D. degree in Xi'an Jiaotong University. His research interest is OTA testing. He received the B.S. degree in Shandong University, Shandong, China, in 2017, and M.S. degree in Northwest Polytechnic University, Xi'an, China, in 2020.



Xiaoming Chen (M'16, SM'19) received the B.Sc. degree in Electrical Engineering from Northwestern Polytechnical University, Xi'an, China, in 2006, and M.Sc. and Ph.D. degrees in Electrical Engineering from Chalmers University of Technology, Gothenburg, Sweden, in 2007 and 2012, respectively. From 2013 to 2014, he was

a Postdoctoral Researcher at the same University. From 2014 to 2017, he was with Qamcom Research & Technology AB, Gothenburg, Sweden, where he was involved in the EU H2020 5GPPP mmMAGIC project (on 5G millimeter-wave wireless access techniques). Since 2017, he has been a Professor at Xi'an Jiaotong University, Xi'an, China. His research areas include 5G multi-antenna techniques, over-the-air (OTA) testing, and reverberation chambers. He has coauthored one book, two book chapter, more than 80 journal papers on these topics. Chen serves as an Associate Editor (AE) for the journal of IEEE Antennas and Wireless Propagation Letters (AWPL). He was also a Guest Editor of a Special Cluster on "5G/6G enabling antenna systems and associated testing technologies" in AWPL and a Special Issue on "Metrology for 5G Technologies" in the journal of IET Microwaves, Antennas & Propagation. He received the URSI (International Union of Radio Science) Young Scientist Awards in 2017 and 2018, and the IEEE outstanding AE awards in 2018 and 2019.



Yingsong Li (M'14-SM'19) received his B.S. degree in Electrical and Information Engineering, and M.S. degree in Electromagnetic Field and Microwave Technology from Harbin Engineering University, 2006 and 2011, respectively. He received his Ph.D. degree from

both Kochi University of Technology (KUT), Japan and Harbin Engineering University, China in 2014. He was a Visiting Scholar of University of California, Davis from March 2016 to March 2017, a visiting Professor of University of York, UK in 2018, a Visiting Professor of Far Eastern Federal University (FEFU) and KUT from 2018. He is a Postdoc of Key Laboratory of Microwave Remote Sensing, Chinese Academy of Sciences from 2016 to 2020. Now, he is a full professor of Harbin Engineering University from July 2014. He is a Fellow of Applied computational Electromagnetics Society (ACES Fellow), and he is also a senior member of Chinese Institute of Electronics (CIE) and a senior member of IEEE. He has authored and coauthored about 300 publications in various areas of electrical engineering, antennas and wireless communications. His current research interests include remote sensing, underwater communications, signal processing, radar, SAR imaging, metasurface designs and microwave antennas.

Li is an Area Editor of AEU-International Journal of Electronics and Communications, and he is an Associate Editor of IEEE Access and Applied Computational Electromagnetics Society Journal (ACES Journal). He is the TPC Co-Chair of the 2019-2020 IEEE International Workshop on Electromagnetics (iWEM 2019), 2019 IEEE 2nd International Conference on Electronic Information and Communication Technology (ICEICT 2019), 2019 International Applied Computational Electromagnetics Society (ACES) Symposium-China, 2019 Cross Strait Quad-regional Radio Science and Wireless Technology Conference (2019 CSQRWC), and iWEM 2020. He also serves as a Session Chair or Organizer for many international conferences, including the WCNC, AP-S, ACES etc. He acts as a Reviewer of numerous IEEE, IET, Elsevier and other international journals.



Juan Chen was born in Chongqing, China, in 1981. She received the Ph.D. degree in Electromagnetic Field and Microwave Techniques at the Xi'an Jiaotong University, Xi'an, China, in 2008. From April 2016 to March 2017, she was a Visiting Researcher in the Department of Electrical and Computer Engineering, Duke University, Durham, NC, under the financial support from the China Scholarship Council. She now serves as a Professor at Xi'an Jiaotong University.

Her research interests are the numerical electromagnetic methods, advanced antenna designs, and graphene theory and application.